Direct generation of time-energy-entangled W triphotons in atomic vapor

Jianming Wen (jianming.wen@gmail.com)
Kennesaw State University https://orcid.org/0000-0003-3373-7108
Yanpeng Zhang (ypzhang@mail.xjtu.edu.cn)
Xi'an Jiaotong University
Yin Cai (caiyin@xjtu.edu.cn)
Xian Jiaotong University, China https://orcid.org/0000-0001-6781-7857
Kangkang Li (kangkang.li@pku.edu.cn)
Xi'an Jiaotong University
Changbiao Li (cbli@mail.xjtu.edu.cn)
Xi'an Jiaotong University
Feng Li (felix831204@xjtu.edu.cn)
Xi'an Jiaotong University https://orcid.org/0000-0003-3533-0184
Zhaoyang Zhang (zhyzhang@mail.xjtu.edu.cn)
Xi'an Jiaotong University
Min Xiao (mxiao@uark.edu)
University of Arkansas https://orcid.org/0000-0002-0718-9518
Saeid Ghamsari (vashahri@gmail.com)
Kennesaw State University

Physical Sciences - Article

Keywords:

DOI: https://doi.org/

Additional Declarations: There is **NO** Competing Interest.

Direct generation of time-energy-entangled W triphotons in atomic vapor

Kangkang Li[1], Jianming Wen[2*], Yin Cai[1*], Saeid Vashahri Ghamsari[2], Changbiao Li[1], Feng Li[1], Zhaoyang Zhang[1], Yanpeng Zhang[1*], and Min Xiao[3,4]
[1]Key Laboratory for Physical Electronics and Devices of the Ministry of Education & Shaanxi Key Lab of Information Photonic Technique, Xi'an Jiaotong University, Xi'an 710049, China
[2]Department of Physics, Kennesaw State University, Marietta, Georgia 30060, USA
[3]National Laboratory of Solid State Microstructures, College of Engineering and Applied Sciences and School of Physics, Nanjing University, Nanjing 210093, China
[4]Department of Physics, University of Arkansas, Fayetteville, Arkansas 72701, USA
*emails: jianming.wen@kennesaw.edu; caiyin@xjtu.edu.cn; ypzhang@mail.xjtu.edu.cn.

Sources of entangled multiphotons are not only essential for fundamental tests of quantum foundations, but are also the cornerstone of a variety of optical quantum technologies today. Over past three decades, tremendous efforts have been devoted to creating multiphoton entanglement by multiplexing existing biphoton sources with linear optics and postselections. Different from all previous protocols, here we report, for the first time, the observation of continuous-mode time-energy-entangled W-class triphotons with an unprecedented generation rate directly through the process of spontaneous six-wave mixing (SSWM) in a four-level triple-Λ atomic vapor cell. Facilitated by electromagnetically induced transparency and coherence control, our SSWM scheme enables versatile narrowband triphoton generation with many intriguing properties including long temporal coherence and controllable waveforms, ideal for implementing long-distance quantum communications, networking, and information processing by interfacing photons and atoms. Most importantly, our work paves a way for the development of a reliable and efficient genuine triphoton source, thus making the research on multiphoton entanglement within easy reach.

Generating entangled multiphoton states[1] is pivotal to probe quantum foundations and advance technological innovations. Comprehensive studies have already shown that multiphoton entanglement[1] enables a plethora of classically impossible phenomena, most of them incomprehensible with any bipartite system. Unfortunately, we hitherto have at hand only biphoton sources based upon spontaneous parametric down-conversion (SPDC) or spontaneous four-wave mixing (SFWM). This has urged tremendous efforts on developing multiphoton sources[1-3] over past thirty years. Among them, the most popular means is to multiplex existing biphoton sources with linear optics and postselections. This brings us the well-known exemplar of polarization-entangled multiphotons[4-8] by constructing imperative interferometric setups. Although postselection might be acceptable in some protocols, it is generally deleterious for most applications since the action of observing photons alters and destroys the states. To avoid postselection, the second path considers cascaded SPDCs/SFWMs[9-12] or two SPDCs/SFWMs followed by one up-conversion[13,14]. In this way, polarization or time-energy entangled triphotons were reported by building sophisticated coincidence counting circuits. Despite no needs on interferometric settings, the attained states are intrinsically non-Gaussian due to unbalanced photon numbers between the primary and secondary biphoton process, thereby making these sources very noisy and inefficient. Alternatively, the third technique[15-17] suggests to coherently mix paired photons with singles attenuated from a cw laser to trigger triphoton events. Akin to the first method, this solution depends on erasing the photon distinguishability by resorting to the Hong-Ou-Mandal interference effect[18]. Though polarization-entangled multiphotons of inequivalent classes were experimented with postselection, the low success rate and required interferometric stabilization make this proposal not so practical. As photons are always emitted in pairs in SPDC/SFWM, this attribute results in the fourth route[19-21] to make use of emission of multiple pairs by appropriately setting input pump powers. Though it seems easy to yield even-number states, yet, dominant biphotons from lower-order perturbation of the parametric process challenge detecting entangled multiphotons from higher-order perturbations. To have an acceptable fidelity, like the second way, a complicated detection system plus an interferometric setup is often inevitable in practice. What's more, this approach mainly allows to form polarization entanglement thus far. In spite of these impressive achievements, all foregoing mechanisms are difficult to offer a reliable and efficient triphoton source for research and applications. Additionally, so far there is no convincing realization of the entangled triphoton experiment in continuous modes. Driven by SPDC, one would expect that such photons could be naturally born from third-order SPDC[22,23] by converting one pump photon of higher energy into three daughter photons of low energy. The idea looks simple and straightforward, but experimentally inaccessible owing to the lack of such a nonlinear optical material. As a result, developing a reliable triphoton source is still in its infancy even up to today.

Coherent atomic media[24], on the other hand, exhibit a wide range of peculiar properties including giant nonlinearities, prolonged atomic coherence, strong photon-atom interaction, and slow/fast light effects. Recently, these exotic properties have been skillfully employed to construct a novel narrowband biphoton source[25-28] basing on SFWM. Specifically, giant nonlinearities promise efficient parametric conversion, long atomic coherence leads to narrowband wavepackets, and sharp optical response becomes a formidable knob for shaping photon waveforms and temporal correlations. Unlike solid state sources, one unique feature pertinent to atomic ensembles arises from the dual role played by the third-order nonlinear susceptibility $\chi^{(3)}$ in biphoton generation[25,29-31]. That is, in addition to governing nonlinear conversion strength, the double-resonance structure in $\chi^{(3)}$ signifies the coexistence of two sets of SFWMs in light quanta radiation. Alternatively, entangled photons output from these two stochastic but coherent SFWM processes interfere and give rise to a nontrivial two-photon interference, namely, the damped Rabi oscillations. In general, their waveforms are entirely patterned by the convolution of a complex phase-mismatch function and $\chi^{(3)}$. Other than these attributes, the nonclassical correlations shared by paired photons can be additionally manipulated by exploiting various coherent control techniques including electromagnetically induced transparency[24] (EIT) to reshape optical responses. The interplay amongst diverse effects also enriches fundamental research and fosters technological innovations, inaccessible to other existing biphoton sources. Besides, flexible system layouts like backward detection geometry are more favorable to photon counting detection. Motivated by these advantages, here we move one step forward and report the direct generation of continuous-mode triphotons entangled in time and energy from a hot atomic vapor cell. By utilizing the process of spontaneous six-wave mixing[32,33] (SSWM), we have not only observed the striking three-photon interference but also witnessed the residual two~photon correlation by tracing one photon out, an intrinsic virtue of the W class of tripartite entanglement[34]. By adjusting the system parameters, we have further achieved waveform-controllable triphoton generation. Together with an unprecedented production rate, our scheme has substantiated to be the first reliable platform that leverages multipartite entanglement research to an unparalleled level.

As schematic in Figs. 1A-C, we are interested in yielding narrowband W triphotons from a 7-cm long ^{85}Rb vapor cell with a four-level triple-Λ atomic configuration at temperature 80°C (or 115°C). The detail of the experimental setup is provided in Methods. In the presence of three counter-propagating cw laser beams (one weak pump $(E_1, \omega_1, \vec{k}_1)$ and two strong couplings $(E_2, \omega_2, \vec{k}_2)$ and $(E_3, \omega_3, \vec{k}_3)$), backward photon triplets $(E_{Sj}, \omega_{Sj}, \vec{k}_{Sj}$ with $j = 1, 2, 3)$ are emitted via Doppler-broadened SSWM at an intersection angle of $\theta \approx 4°$ to the principle z-axis along the phase matching direction, $\Delta\vec{k} = \left(\vec{k}_{S1} + \vec{k}_{S2} + \vec{k}_{S3}\right) - (\vec{k}_1 + \vec{k}_2 + \vec{k}_3) = 0$. As depicted in Figs. 1B and C, the three coaxial input lasers were coupled into the center of the ^{85}Rb vapor cell with tunable frequency detunings Δ_j and powers P_j; while the generated photon triplets were accordingly detected by three single-photon counting modules ($SPCM_1$ – $SPCM_3$) for coincidence counts after spatial and frequency filtering. Here, to avoid unwanted accidental trigger events induced by singles and dual biphotons, we placed single-band filters and narrowband etalon Fabry-Perot cavities in front of $SPCM_j$ before detection. We notice that in three-photon joint clicks, the major source of accidental coincidences stems from double pairs from two different SFWMs simultaneously present in the detection system (Supplementary Information (SI)). Since these dual pairs may have similar central frequencies and polarizations as genuine triphoton modes, they cannot be filtered away simply by polarizers and frequency filters. To exclude such double-pair false trigger events, in experiment we further introduced an additional $SPCM_d$ synchronized with $SPCM_3$ to serve as the diagnosis detector in conjunction with the rest two, $SPCM_1$ and $SPCM_2$. To ensure the atomic population to be mainly distributed in the ground level $\left|5S_{\frac{1}{2}}, F = 2\right\rangle$ throughout the measurement, an additional strong optical repumping beam (E_{op}) was applied to the atomic transition $\left|5S_{\frac{1}{2}}, F = 3\right\rangle \rightarrow \left|5P_{\frac{1}{2}}\right\rangle$ in alignment with E_2 but without spatial overlap. With these preparations, we carefully adjust the system parameters, especially P_j and Δ_j of each input field E_j, to promote the SSWM occurrence.

Physically, the SSWM process can be understood from the effective interaction Hamiltonian

$$H = \epsilon_0 \int_V d^3r \chi^{(5)} E_1 E_2 E_3 E_{S1}^{(-)} E_{S2}^{(-)} E_{S3}^{(-)} + H.c.\ (H.c., \text{Hermitian conjugate}), \quad (1)$$

with three input (output) beams treated as classical (quantized) fields and V being the interaction volume. In Eq. (1), $\chi^{(5)}$ denotes the fifth-order Doppler-broadened nonlinear susceptibility and governs the nonlinear conversion efficiency. In the Schrödinger picture, after some algebra, the triphoton state at the two cell surfaces can be derived from first-order perturbation theory by ignoring the vacuum contribution (SI), and takes the form of

$$|\Psi\rangle \propto \iiint d\omega_{S1} d\omega_{S2} d\omega_{S3} \chi^{(5)} \Phi\left(\frac{\Delta k L}{2}\right) \delta(\Delta\omega) \left|1_{\omega_{S1}}, 1_{\omega_{S2}}, 1_{\omega_{S3}}\right\rangle. \quad (2)$$

Here, $\Delta\omega = \sum_{j=1}^{3}(\omega_{Sj} - \omega_j)$, L is the interaction length, $\Delta k = \Delta\vec{k} \cdot \hat{z}$ is the phase (or wavenumber) mismatch, the phase-mismatch longitudinal function $\Phi(x) = \mathrm{sinc}(x)e^{-ix}$ ascribes the three-photon natural spectral width arising from their different group velocities. Besides conditioning the triphoton output rate, the $\chi^{(5)}$-resonance profile also specifies the generation mechanism along with the photon intrinsic bandwidths. Overall, the state (2) outlines a few peculiar features yet to be experimentally verified: First, because of its non-factorization, $|\Psi\rangle$ is entangled in frequency (or time), instead of polarization. Second, characterized by two independent variables, $|\Psi\rangle$ conforms to the essential characteristics of the tripartite W class, that is, by tracing one photon away, partial entanglement still exists in the remaining bipartite subsystem. Third, since the triphoton waveform is defined by the convolution of Φ and $\chi^{(5)}$, two distinct types of Glauber third-order (as well as conditional second-order) temporal correlations are expected to be manifested in threefold (and conditioned twofold) coincidence counting measurement. Consequently, two very differing scenarios are expected to be revealed in triphoton coincidence counting measurement. Last, but not the least, the triplet production rate is linear in the intensity of each input laser and can be dramatically enhanced by orders of magnitude by optimizing system parameters. It is worth pointing out that all these striking properties have been well affirmed in our series of experiments. Of importance, this is the first experimental proof of the time-energy-entangled triphoton W state discovered a decade ago[34] but never realized.

In experiment, we optimized the SSWM phase-matching condition via controlling the frequency detunings and incident angles of three driving fields so as to effectively collect emitted triphotons. Upon triggering $SPCM_j$, the temporal correlation was concealed in photon counting histograms saved in a fast-time acquisition card with 0.0244-ns bin width, where, within in every time window of 195 ns, the detection of an E_{S1}-photon triggered the start of a coincidence event that ended with the detection of subsequent E_{S2}- and E_{S3}-photons. In most measurements, we collected the total trigger events over an hour and then analyzed the corresponding three-photon coincidences from the histogram in the parameter space (τ_{21}, τ_{31}), where $\tau_{21} = \tau_2 - \tau_1$ and $\tau_{31} = \tau_3 - \tau_1$ are respectively the relative time delays with τ_j being the triggering time of the $SPCM_j$.

As an exemplar of such, Fig. 2A displays one set of measured threefold coincidence counts from one recorded histogram after subtracting the accidental noise, giving rise to an intriguing three-dimensional temporal correlation with the 18.6- and 19.0-ns effective measurement time window along the τ_{21}- and τ_{31}-axis because of the employed dectors. For the 0.25-ns time-bin width per detector, integrating all involved time bins yields the total of ~6×10^3 threefold trigger events, which result in a raw triphoton generation rate of 102 ± 9 per minute without account of the coupling loss and detection efficiency. This rate is orders of magnitude higher than any previous one, and can be further improved by applying more efficient SPCMs as well as optimizing the fiber coupling efficiency. From the raw data, the background accidentals were estimated to be 6 ± 1 per minute, mainly originating from the residual dual pairs as well as accidental coincidences of uncorrelated singles and dark counts of the SPCMs. This low background noise implies that the undesired third-order nonlinear processes were well filtered out in the experiment. On the other hand, the complicated pattern is a direct consequence of nontrivial W-triphoton interferences due to the occurrence of multiple coexisting SSWM processes in the regime of damped Rabi oscillations. As described previously, these processes arise from the multi-resonance structure of $\chi^{(5)}$. According to our dressed-state calculations (SI), there are four such coexisting channels, as schematic in Fig. 2B, coherently contributing to the observed quantum interference. To confirm that the emitted triphoton state belongs to the W class, we then used the acquired data to investigate the correlation properties of different bipartite subsystems. To do so, we integrated the coincidence counts by tracing away one photon from every triphoton event over that photon's arrival time. In this way, we acquired the conditional two~photon temporal waveforms with τ_{21} or τ_{31} as variables, and plotted them, respectively, in Figs. 2C and D. Interestingly, the conditioned τ_3-waveform in Fig. 2D exhibits a damped periodic oscillation with a period of ~6.2 ns (SI); while the τ_{21}-waveform in Fig. 2C reveals two superimposed damped periodic oscillations with another 1.7-ns period in addition to the 6.2-ns one (SI), an interference effect unusual to any existing biphoton source. In contrast, the triphoton waveform has flexible temperal widths, for instance, 28 ns along the direction of $\tau_{21} + \tau_{31} = 15$ ns (Fig. 2E). This contrasting phenomenon also supports our theoretical picture from alternative aspect, that the observed interference is caused by at least three sets of coherently coexisting SSWM processes. As demonstrated in SI, our qualitative analysis gives a good account of the experimental data.

Since the attributes of triphoton waveforms are dependent on the system parameters, this prompts us to manipulate and control their quantum correlations by means of tuning the input lasers as well as the atomic density or optical depth (OD). To this end, we carried out a series of experiments to tailor temporal correlation by shaping their waveforms by varying various parameters. Two sets of such representative experimental data are presented in Fig. 3. In comparison to Fig. 2A, Fig. 3A shows the steered waveform by reducing the power and frequency detuning of the input E_2 laser. As one can see, the profile of the triphoton temporal correlation is dramatically changed in spite of the reduced generation rate 77.4 ± 7.8 minute^{-1}. Especially, the conditional two~photon coincidence counts manifest mono-periodic oscillations with the same period of 6.2 ns along both τ_{21} and τ_{31} directions, as illustrated in Figs. 3B and C. This is because, in this case, the Rabi frequency of E_2 was tuned to be very close to that of E_3. As a consequence, half of the multiple resonances associated with the emission of E_{S2}-photons (Fig. 2B) become degenerate and share the same spectrum. Likewise, the triphoton temporal coherence length along the $\tau_{21} + \tau_{31} = 29$ ns direction is enlarged to 40 ns. On the other hand, triphoton interference can be also modulated by altering the phase-mismatch longitudinal function Φ in Eq. (2). Akin to the biphoton generation, the phase mismatch Δk in Φ is determined by the linear susceptibility of each mode in SSWM via the EIT slow-light effect. As showcased in Fig. 3D, by augmenting the OD from 4.6 to 45.7, the triphoton temporal correlation is considerably modified by the dispersion relation of the atomic vapor and falls into the group-delay regime. In addition to raising the production rate to 125 ± 11 per minute, the oscillatory curvature is markedly suppressed and replaced by the overall decay envelopes. This transformation becomes more evident when examining the conditioned two~photon coincidence counts. By comparing Fig. 3F with Figs. 3B, C and E, one can see that the enhanced dispersion apparently smears the damped Rabi oscillations along the τ_{21}-direction, implying that the narrower bandwidths defined by $\Phi\left(\frac{\Delta kL}{2}\right)$ regulate the bandwidths dictated by $\chi^{(5)}$ to obscure the interference amongst four sets of coexisting SSWM channels. Besides, the triphoton temporal coherence length along the direction of $\tau_{21} + \tau_{31} = 50$ ns is also significantly prolonged up to 70 ns.

To reveal the nonclassicality of the W triphoton state, we continued to examine the violation of the Cauchy-Schwarz inequality[35,36] as well as the fringe visibilities of the observed Rabi oscillations. By normalizing the threefold coincidence events to the flat background counts along with the additional auto-correlation measurement of the collected E_{S1}, E_{S2} and E_{S3} photons, we found that the Cauchy-Schwarz inequality is violated by a factor of 250 ± 55 in Fig. 2A, 154 ± 43 in Fig. 3A, and 79 ± 21 in Fig. 3D. Note that here these values were optimized by filtering possible biphoton processes in measurement. Additionally, we observed that the fringe visibility of Fig. 2A can be as high as $90 \pm 5\%$.

In addition to the above experiments, it is also instructive to explore the triphoton production rate and temporal correlation width as a function of the input pump power for further understanding the proposed generation mechanism. This has motivated us to implement additional measurements and the experimental data is presented in Fig. 4. As one can see, indeed, the triphoton generation rate follows a linear growth in the input power P_2 of the E_2 field. For the temporal coherence length, we concentrated on the two~photon conditional coincidence counting along the τ_{21} and τ_{31} directions. From Fig. 4, it is not difficult to find that increasing P_2 results in the reduction of the correlation time. This stems from the reduced slow-light effect when augmenting P_2. Note that Figs. 2A, 3A and 3D simply become one individual point in Fig. 4. Overall, our approach enables all-optical coherent manipulation to create the genuine triphotons with controllable waveforms.

In conclusion, we have for the first time observed the efficient W-triphoton emission directly through SSWM in a warm atomic vapor with a generation rate of about 125 ± 11 min^{-1}. Moreover, due to the coexistence of multi-SSWMs, these time-energy-entangled W triphotons have resulted in various nontrivial three-photon temporal interferences. Furthermore, by manipulating the system parameters, the triphoton temporal correlations can be flexibly engineered and tailored and demonstrate many peculiar characteristics inaccessible to all previous mechanisms. As a reliable source, it is expected to play a vital role in probing foundations of quantum theory and advancing various quantum-based technologies in information processing, communications, imaging, metrology, etc.

References

1. Pan, J.-W., Chen, Z.-B., Lu, C.-Y., Weinfurter, H., Zeilinger, A. & Zukowski, M. Multiphoton entanglement and interferometery. *Rev. Mod. Phys.* **84**, 777-838 (2012).
2. Friis, N., Vitagliano, G., Malik, M. & Huber, M. Entanglement certification from theory to experiment. *Nat. Rev. Phys.* **1**, 72-87 (2019).
3. Erhard, M., Krenn, M. & Zeilinger, A. Advances in high-dimensional quantum entanglement. *Nat. Rev. Phys.* **2**, 365-381 (2020).
4. Bouwmeester, D., Pan, J.-W., Daniell, M., Weinfurter, H. & Zeilinger, A. Observation of three-photon Greenberger-Horne-Zeilinger entanglement. *Phys. Rev. Lett*. **82**, 1345-1349 (1999).
5. Pan, J.-W., Bouwmeester, D., Gasparoni, S., Weihs, G. & Zeilinger, A. Experimental demonstration of four-photon entanglement and high-fidelity teleportation. *Phys. Rev. Lett.* **86**, 4435-4439 (2001).
6. Eibl, M., Kiesel, N., Bourennane, M., Kurtsiefer, C. & Weinfurther, H. Experimental realization of a three-qubit entangled W state. *Phys. Rev. Lett.* **92**, 077901 (2004).
7. Kiesel, N., Schmid, C., Toth, G., Solano, E. & Weinfurther, H. Experimental observation of four-photon entangled Dicke state with high fidelity. *Phys. Rev. Lett.* **98**, 063604 (2007).
8. Reimer, C., Kues, M., Roztocki, P., Wetzel, B., Grazioso, F., Little, B. E., Chu, S. T., Johnson, T., Bromberg, Y., Caspani, L., Moss, D. J. & Morandotti, R. Generation of multiphoton entangled quantum states by means of integrated frequency combs. *Science* **351**, 1176-1180 (2016).
9. Wen, J., Oh, E. & Du, S. Tripartite entanglement generation via four-wave mixings: narrowband triphoton W state. *J. Opt. Soc. Am. B* **27**, A11-A20 (2010).
10. Hubel, H., Hamel, D. R., Fedrizzi, A., Ramelow, S., Resch, K. J. & Jennewein, T. Direct generation of photon triplets using cascaded photon-pair sources. *Nature* **466**, 601-603 (2010).
11. Shalm, L. K., Hamel, D. R., Yan, Z., Simon, C., Resch, K. J. & Jennewein, T. Three-photon energy-time entanglement. *Nat. Phys*. **9**, 19-22 (2013).
12. Hamel, D. R., Shalm, L. K., Hubel, H., Miller, A. J., Marsili, F., Verma, V. B., Mirin, R. P., Nam, S. W., Resch, K. J. & Jennewein, T. Direction generation of three-photon polarization entanglement. *Nat. Photon.* **8**, 801-807 (2014).
13. Keller, T. E., Rubin, M. H., Shih, Y. & Wu, L.-A. Theory of the three-photon entangled state. *Phys. Rev. A* **57**, 2076-2079 (1998).
14. Wen, J., Xu, P., Rubin, M. H. & Shih, Y. Transverse correlations in triphoton entanglement: Geometrical and physical optics. *Phys. Rev. A* **76**, 023828 (2007).

15. Rarity, J. & Tapster, P. Three-particle entanglement from entangled photon pairs and a weak coherent state. *Phys. Rev. A* **59**, R35-R38 (1999).
16. Zhao, Z., Chen, Y.-A., Zhang, A.-N., Yang, T., Briegel, H. J. & Pan, J.-W. Experimental demonstration of five-photon entanglement and open destination teleportation. *Nature* **430**, 54-58 (2004).
17. Mikami, H., Li, Y., Fukuoka, K. & Kobayashi, T. New high-efficiency source of a three-photon W state and its full characterization using quantum state tomography. *Phys. Rev. Lett.* **95**, 150404 (2005).
18. Hong, C. K., Ou, Z. Y. & Mandel, L. Measurement of subpicosecond time intervals between two photons by interference. *Phys. Rev. Lett*. **59**, 2044-2046 (1987).
19. Eibl, M., Gaertner, S., Bourennane, M., Kurtsiefer, C., Zukowski, M. & Weinfurther, H. Experimental observation of four-photon entanglement from parametric down-conversion. *Phys. Rev. Lett.* **90**, 200403 (2003).
20. de Riedmatten, H., Scarani, V., Marcikic, I., Acin, A., Tittel, W., Zbinden, H. & Gisin, N. Two independent photon pairs versus four-photon entangled states in parametric down conversion. *J. Mod. Opt.* **51**, 1637-1649 (2003).
21. Bourennane, M., Eibl, M., Gaertner, S., Kurtsiefer, C., Cabello, A. & Weinfurther, H. Decoherence-free quantum information processing with four-photon entangled states. *Phys. Rev. Lett.* **92**, 107901 (2004).
22. Corna, M., Garay-Palmett, K. & U'Ren, A. B. Experimental proposal for the generation of entangled photon triplets by third-order spontaneous parametric downconversion. *Opt. Lett.* **36**, 190-192 (2011).
23. Borshchevskaya, N. A., Katamadze, K. G., Kulik, S. P. & Fedorov, M. V. Three-photon generation by means of third-order spontaneous parametric down-conversion in bulk crystals. *Laser Phys. Lett.* **12**, 115404 (2015).
24. Fleischhauer, M., Imamoglu, A. & Marangos, J. P. Electromagnetically induced transparency: Optics in coherent media. *Rev. Mod. Phys.* **77**, 733-673 (2005).
25. Du, S., Wen, J. & Rubin, M. H. Narrowband biphoton generation near atomic resonance. *J. Opt. Soc. Am. B* **25**, C98-C108 (2008).
26. Balic, V., Braje, D. A., Kolchin, P., Yin, G. Y. & Harris, S. E. Generation of pairs photons with controllable waveforms. *Phys. Rev. Lett*. **94**, 183601 (2005).
27. Du, S., Kolchin, P., Belthangady, C., Yin, G. Y. & Harris, S. E. Subnatural linewidth biphotons with controllable temporal length. *Phys. Rev. Lett.* **100**, 183603 (2008).
28. Shu, C., Chen, P., Chow, T. K. A., Zhu, L., Xiao, Y., Loy, M. M. T. & Du, S. Subnatural-linewidth biphotons from a Doppler-broadended hot atomic vapor cell. *Nat. Commun.* **7**, 12783 (2016).
29. Wen, J., Du, S. & Rubin, M. H. Biphton generation in a two-level atomic ensemble. *Phys. Rev. A* **75**, 033809 (2007).
30. Wen, J., Du, S. & Rubin, M. H. Spontaneous parametric down-conversion in a three-level system. *Phys. Rev. A* **76**, 013825 (2007).

31. Wen, J., Du, S., Zhang, Y., Xiao, M. & Rubin, M. H. Nonclassical light generation via a four-level inverted-Y system. *Phys. Rev. A* **77**, 033816 (2008).
32. Kang, H., Hernandez, G. & Zhu, Y. Slow-light six-wave mixing at low light intensities. *Phys. Rev. Lett.* **93**, 073601 (2004).
33. Zhang, Y., Brown, A. W. & Xiao, M. Opening four-wave mixing and six-wave mixing channels via dual electromagnetically induced transparency windows. *Phys. Rev. Lett.* **99**, 123603 (2007).
34. Wen, J. & Rubin, M. H. Distinction of tripartite Greenberger-Horne-Zeilinger and W states entangled in time (or energy) and space. *Phys. Rev. A* **79**, 025802 (2009).
35. Reid, M. D. & Walls, D. F. Violations of classical inequalities in quantum optics. *Phys. Rev. A* **34**, 1260-1276 (1986).
36. Belinskii, A. V. & Klyshko, D. N. Interference of light and Bell's theorem. *Phys.-Usp.* **36**, 653-693 (1993).

Acknowledgements

We are grateful to Xinghua Li, Dan Zhang, and Da Zhang for their contributions at the early stage of the project and to Yanhua Zhai for helpful discussions on the detection system. This research was supported by the National Key Research and Development Program of China (2017YFA0303700, 2018YFA0307500), Key Scientific and Technological Innovation Team of Shaanxi Province (2021TD-56), National Natural Science Foundation of China (61975159, 12174302, 62022066, 12074306, 12074303).

Author Contributions

Y.Z. and J.W. conceived the idea and supervised the project with the help from Y.C. K.L., supervised by J.W. and Y.Z., performed the experiment, theoretical derivations, and numerical calculations with the help from S.V.G. J.W., K.L. and Y.Z. wrote the manuscript with contributions from all other authors. All contributed to the discussion of the project and analysis of experimental data.

Additional Information

Supplementary information is available in the online version of the paper. Reprints and permissions information is available online at www.nature.com/reprints. Correspondence and requests for materials should be addressed to J.W., Y. Z. or C.Y.

Competing financial interests

The authors declare no competing financial interests.

List of Figures

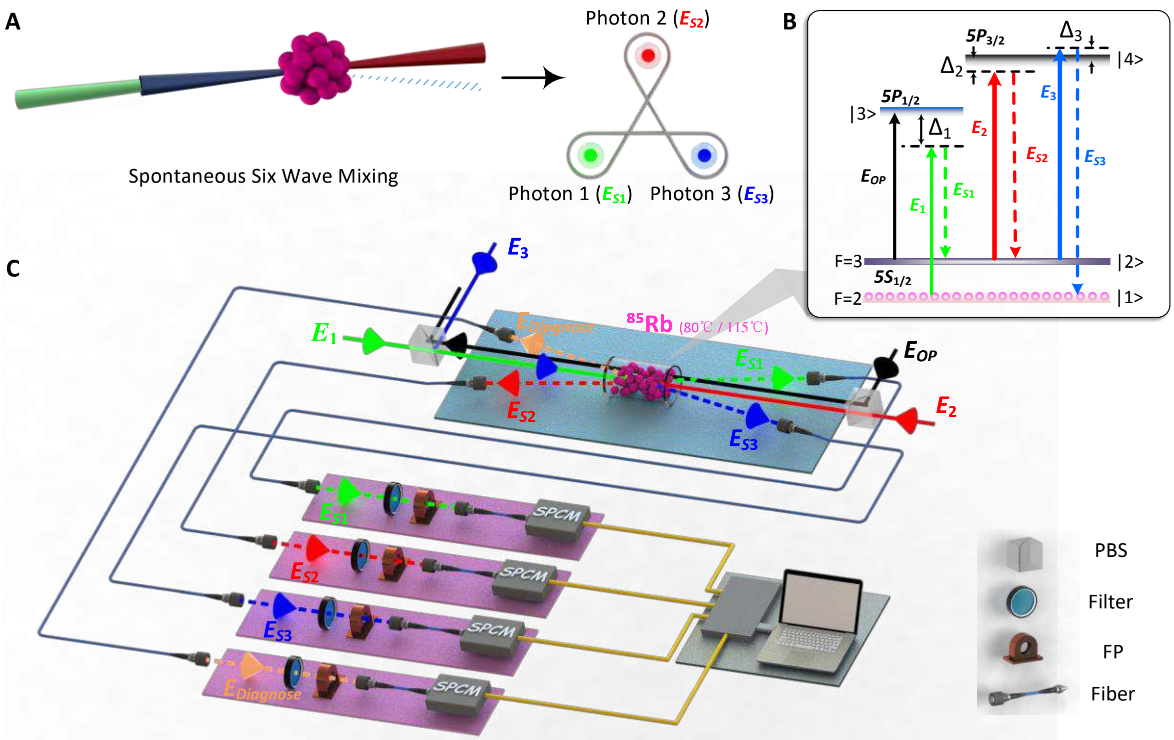

Fig. 1. Generation of genuine W-triphotons entangled in time-energy directly via SSWM in a hot atomic vapor. (**A**) Conceptual schematic of creating a W-triphoton state via the fifth-order parametric nonlinear process. (**B**) The ^{85}Rb energy-level diagram of the SSWM process. (**C**) The experimental setup. Three coaxial input driving fields E_1 (795 nm), E_2 (780 nm) and E_3 (780 nm) are coupled into the center of an ^{85}Rb vapor cell heated at 80°C (or 115°C) to initiate the simultaneous generation of W-triphotons in E_{S1}, E_{S2} and E_{S3}. An additional optical-pumping beam E_{OP} is added to clean up the residual atomic population in the level |2> for preventing the noise from the Raman scattering. The generated photons are coupled into a data acquisition system by single-mode fibers and jointly detected by three synchronized single-photon counting modules (SPCM) with filters (F) and Fabry–Perot cavities (FP) placed in front. To eliminate accidental coincidences caused by dual biphotons and quadraphotons, an extra detection of the diagnosis photons E_{Diagnose} is applied to ensure the natural triphoton collection. All trigger events are then interrogated by a fast-time acquisition card with a computer.

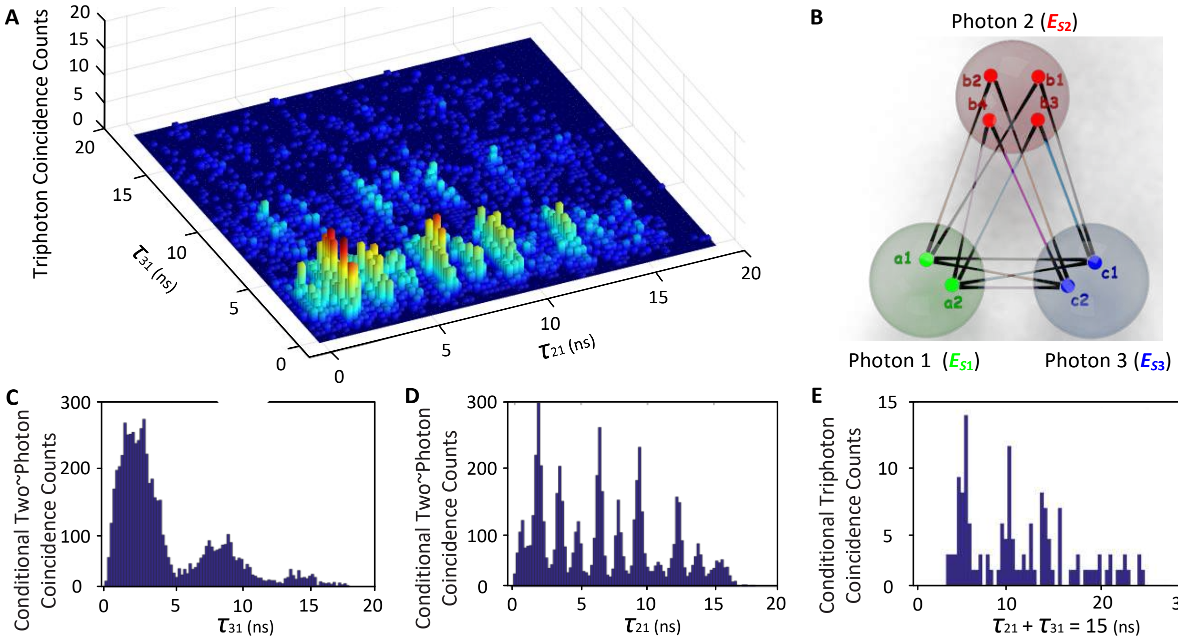

Fig. 2. Triphoton coincidence counting measurements. (**A**) Three-dimensional (3D) quantum interference formed by three-photon coincidence counts collected in 1 h with the time-bin width of 0.25 ns for OD = 4.6. The generation rate and accidentals are respectively 102 ± 9 and 6 ± 1 per minute. The powers of the input E_1, E_2 and E_3 beams are $P_1 = 4$ mW, $P_2 = 40$ mW, and $P_3 = 15$ mW, respectively, and the corresponding frequency detunings are $\Delta_1 = -2$ GHz, $\Delta_2 = -150$ MHz, and $\Delta_3 = 50$ MHz. (**B**) Schematic illustration of triphoton interference originating from the coexistence of multi-SSWMs. (**C**) & (**D**) Conditional two~photon coincidence counts as the function of τ_{21} and τ_{31} in (**A**) by tracing the third photon E_{S3} and E_{S2}, respectively. (**E**) Conditional three-photon coincidence counts along the trajectory of $\tau_{21} + \tau_{31} = 15$ ns in (**A**).

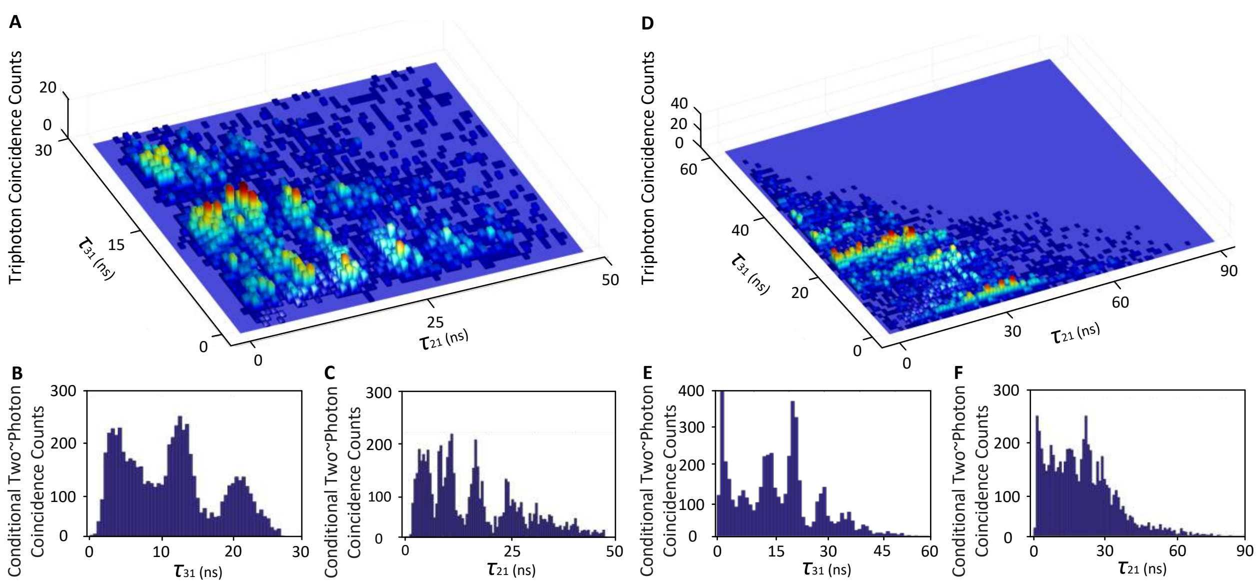

Fig. 3. Triphoton coincidence counting measurements by tuning the coupling strength and OD. (**A**) 3D quantum interference formed by three-photon coincidence counts collected in 1h with the 0.7-ns time-bin width by changing P_2 to 15 mW and Δ_2 to -50 MHz. Other parameters are same as Fig. 2. The generation rate and accidentals rate are 77.4 ± 7.8 and 11 ± 2.1 per minute, respectively. (**B**) & (**C**) Conditional two~photon coincidence counts as the function of τ_{21} and τ_{31} in (**A**) by tracing the third photon E_{S3} and E_{S2}, respectively. (**D**) Collected over 40 min with 1-ns time-bin width by changing OD to 45.7. Other parameters are same as Fig. 2. The generation and accidentals rates are 125 ± 11 and 28 ± 6.4 per minute, respectively. (**E**) & (**F**) Conditional two~photon coincidence counts as the function of τ_{21} and τ_{31} in (**D**).

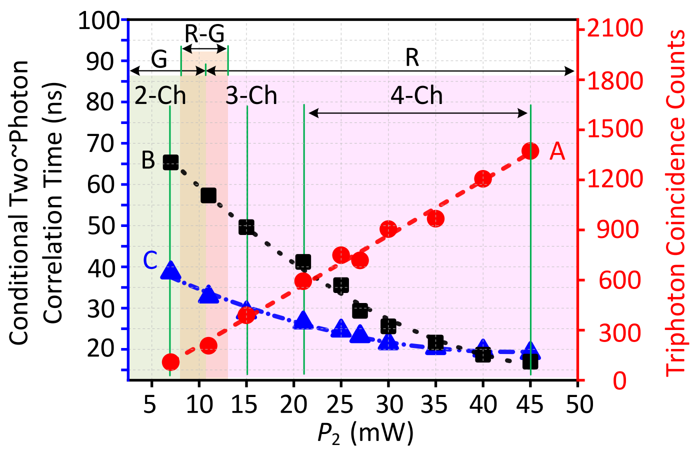

Fig. 4. Controllable waveform generation. The triphoton generation rate (red dots) in 15 minutes versus the input power P_2 of the driving field E_2. The correlation times of conditional two~photon coincidences along the τ_{21} (black squares) and τ_{31} (blue triangles) directions by changing P_2. By increasing P_2, the triphoton temporal correlation is shifted from the group-delay (G) regime to the Rabi-oscillation (R) region. j-Ch ($j = 2,3,4$) means the coherent coexistence of j types of indistinguishable SSWMs. The experimental condition is same as that in Fig 2.

Methods

Experimental implementation. Experimentally, three coaxial driving beams E_1, E_2 and E_3 are coupled to the center of the ^{85}Rb vapor cell to initiate the SSWM process, as shown in Fig. 2. The relevant energy-level diagram is shown in Fig. 1B, where the atoms are prepared at the ground level $|1\rangle$ $(5S_{1/2}, F = 2)$. The other involved energy levels are $|2\rangle$ $(5S_{1/2}, F = 3)$, $|3\rangle$ $(5P_{1/2})$, and $|4\rangle$ $(5P_{3/2})$. The horizontally polarized weak probe E_1 beam at the 795-nm wavelength is applied the atomic transition $|1\rangle \rightarrow |3\rangle$ with a large red frequency detuning Δ_1 (2 GHz) so that the atomic population resides primarily at $|1\rangle$. The other two strong coupling beams E_2 (780 nm, horizontal polarization) and E_3 (780 nm, vertical polarization) are near resonantly coupled to the same atomic transition $|2\rangle \rightarrow |4\rangle$ but with changeable detunings Δ_2 and Δ_3. By carefully adjusting the phase matching conditions, the spatially separated triphotons E_{S1}, E_{S2} and E_{S3} with wave vectors $\vec{k}_{S1}$, $\vec{k}_{S2}$ and $\vec{k}_{S3}$ are spontaneously emitted along the phase-matching directions with a small forward angle about 4° away from the three driving fields. Besides, we have added an additional optical-pumping beam E_{OP} to clean up the residue atomic population in $|2\rangle$ so that the Raman scattering can be suppressed from the transition $|2\rangle \rightarrow |3\rangle$. To increase the fifth-order nonlinearity, the ^{85}Rb vapor cell with a length of $L = 7$ cm is heated to 80°C (or 115°C). In this regard, the reported data in Figs. 2 and 3A-C were collected at the temperature of 80°C; while the data presented in Figs. 3D-F were obtained at 115°C. Also, the narrowband filters and customized interference etalon Fabry-Perot (FP) cavities are placed in front of each SPCM to filter the scattered driving lasers from the collected triphoton trigger events. After detected by SPCMs, the trigger events are recorded by a time-to-digit converter, where the maximum resolution time of our recording card is 813 fs. In our experiment, the fiber-fiber coupling efficiency and the SPCM detection efficiency are 70% and 40%, respectively.

Filtering possible biphoton processes from triphoton coincidence counts. Although the triphoton generation by SSWM is the focus of the measurement, due to the larger magnitude of the third-order nonlinearity, it is necessary to consider the possible false counts from the biphoton processes. Based on the atomic level structure and the adopted field coupling geometry, there are seven crucial SFWMs (Fig. S6 in SI) that may result in accidental coincidences: (1) SFWM1 initiated by E_1 and E_2, (2) SFWM2 by E_1 and E_3, (3) SFWM3 by E_2 and E_3, (4) SFWM4 by E_3 and E_2, (5) SFWM5 by $2E_1$, (6) SFWM6 by $2E_2$, and (7) SFWM7 by $2E_3$. Specifically, the biphotons produced from the following SFWMs may contribute to the accidental joint-detection probability: (1) SFWM1 + SFWM2, (2) SFWM1 + SFWM3, (3) SFWM1 +SFWM4, (4) SFWM1 + SFWM5, (5) SFWM1 + SFWM7, (6) SFWM2 + SFWM3, (7) SFWM2 + SFWM4, (8) SFWM2 + SFWM6, (9) SFWM3 + SFWM4, (10), SFWM3 + SFWM5, (11) SFWM3 + SFWM7, (12) SFWM4 + SFWM5, (13) SFWM4 + SFWM7, (14) SFWM5 + SFWM6, and (15) SFWM6 +SFWM7. Fortunately, the central frequency difference of the similar photons from SSWM and SFWMs are more than 3 GHz. Therefore, before being detected by SPCMs, the collected photons need to pass through the high-quality single-frequency band filters and the customized narrowband etalon Fabry-Perot cavity (with a bandwidth ~600 MHz). The bandwidth, transmission efficiency, and extinction ratio of the employed filters are 650 MHz, 80%, and 60 dB, respectively. After these measures, most of the biphoton noise can be filtered from the detection. In addition, the phase-matching condition for the SSWM process is much different from those for the possible SFWM processes. For instance, the photons from SFWM2 have distinctive emission angles from those from SSWM. As a result, the three-photon coincidence counts in actual measurements are mainly determined by true triphotons, uncorrelated singles, and dark counts. In practice, the biphotons and uncorrelated singles can be well filtered in the three-photon coincidence counting measurement by carefully adjusting the phase-matching conditions.

Additional detection of diagnose photons $E_{\mathbf{Diagnoise}}$. To further guarantee the detected photons that are really from SSWM, we have performed one additional detection of the two-photon coincidences E_{S3} and E_{Diagnose} simultaneously in conjunction with the coincidences between E_{S1} and E_{S2} by artificially introducing the diagnose photons E_{Diagnose}. This arrangement allows us to greatly reduce the false three-photon trigger events from dual biphotons particularly. The experimental results of E_{S3} and E_{Diagnose} are given in the SI. By the same reconstruction method, we notice that the trigger events from two pairs of biphotons can be safely removed from the data recording.

The Cauchy-Schwarz inequality. The nonclassicality of triphoton correlation can be verified by observing the violation of the well-known Cauchy-Schwarz inequality, which is defined by

$$\frac{\left[g^{(3)}(\tau_{21},\tau_{31})\right]^2}{\left[g_{S1}^{(1)}\right]^2\left[g_{S2}^{(1)}\right]^2\left[g_{S3}^{(1)}\right]^2} \leq 1.$$

Here, $g^{(3)}(\tau_2,\tau_3)$ is the normalized third-order correlation function with respect to the accidental background. $g_{S1}^{(1)}$, $g_{S2}^{(1)}$ and $g_{S3}^{(1)}$ are the normalized autocorrelations of the emitted photons E_{S1}, E_{S2} and E_{S3} measured by a fiber beam splitter. In our experiment, the nonzero background floor in such as Figs. 2 and 3 is a result of the accidental coincidences between uncorrelated single photons. According to the measured data, we estimate that the maximum values of $g_{S1}^{(1)}$, $g_{S2}^{(1)}$ and $g_{S3}^{(1)}$ are respectively to be 1.6 ± 0.2, 2 and 2.

Supplementary Files

This is a list of supplementary files associated with this preprint. Click to download.

- SupplementaryInformation0210.pdf